JOURNAL OF PROPULSION AND POWER
Vol. 27, No. 2, March–April 2011

Theoretical Investigation of the Influence of Constriction and Combustion on Ejector Performance

M. Koupriyanov* and J. Etele*
Carleton University, Ottawa, Ontario K1S 5B6, Canada

DOI: 10.2514/1.B34025

A theoretical analysis of a variable area ejector with and without combustion is presented. The flowfield is solved using a steady, quasi-one-dimensional, inviscid control volume formulation with combustion effects included via a generalized equilibrium calculation. Results for the compression augmentation due to area constriction in a nonreacting ejector flowfield show good agreement between theoretical predictions and numerical simulations using an approximate wall pressure distribution that does not require experimental data. Compression augmentation is shown to be sensitive to the equivalence ratio within the primary rocket chamber, where ejector performance is greatest at both low and high equivalence ratios but near a minimum at stoichiometric conditions. For an axisymmetric ejector with a 15% decrease in area along its length at an equivalence ratio of 2.5, the compression factor obtained can be increased by over 14% when compared with a straight ejector with the primary rocket operating at nominal conditions.

Nomenclature

A	=	area
a	=	speed of sound
C_p	=	specific heat at constant pressure
C_R	=	Contraction ratio $1 - A_m/A_i$
$\bar{h}$	=	molar enthalpy
h^o	=	specific total enthalpy, $(h + u^2/2)$
$\bar{h}_f$	=	molar standard heat of formation
L	=	length of ejector duct
M	=	Mach number
$\dot{m}$	=	mass flow rate
N	=	molar flow rate
p	=	pressure
R	=	gas constant
R_u	=	universal gas constant
T	=	temperature
W	=	molecular weight
x	=	axial distance
Y	=	mass fraction
α	=	air/rocket mass flow ratio
γ	=	ratio of specific heats
θ	=	air/rocket specific total enthalpy ratio
π_m	=	compression ratio, p_m^o/p_a^o
$\bar{\pi}_m$	=	compression augmentation, $\pi_m/[\pi_m]_{C_R=0}$
σ	=	rocket exhaust/ejector inlet area ratio
ϕ	=	rocket equivalence ratio

Subscripts

a	=	air
i	=	ejector inlet
k	=	species
m	=	mixed flow (ejector exit)
r	=	rocket
ref	=	reference conditions (273 K, 1 atm)
w	=	wall
2	=	point of maximum expansion

Superscripts

o	=	stagnation conditions
$*$	=	sonic conditions

Received 25 May 2010; revision received 21 September 2010; accepted for publication 12 November 2010.

*Mechanical and Aerospace Engineering.

Introduction

CURRENTLY the only available means of orbital insertion is by using chemical rocket engines. Although rocket propulsion offers a high thrust-to-weight ratio, it suffers from a relatively low specific impulse (on the order of 300 s), as well as the burden of having to carry a large quantity of onboard oxidizer. A promising alternative is the so-called combined-cycle propulsion system (CCP), which integrates different propulsive cycles into a single engine/flowpath architecture. One of the variants of the CCP system is the rocket-based combined-cycle (RBCC), which has at its core a chemical rocket. A RBCC engine typically operates in four flight modes, namely the rocket ejector mode, the ramjet mode, the scramjet mode, and finally a pure rocket mode. The multimode operation of the engine is where it draws most of its benefits since each propulsive cycle can be used at its optimum operating conditions (altitude and Mach number). More detail on RBCC operation as well as a summary of technical issues can be found in Daines and Segal [1].

Given the inherent advantages of such an engine significant research has been carried out in the field dating back to the work of von Karman [2]. The focus of the majority of this work has been on the low-speed ejector mode. In this mode, the pumping action of the rocket stream entrains and compresses atmospheric air through a turbulent mixing process. To exploit the incoming supply of fresh oxygen and further enhance thrust extra fuel can be added by either running the rocket fuel rich and operating the ejector in the simultaneous mixing and combustion (SMC) scheme, or by allowing both streams to mix first and injecting extra fuel further downstream thereby operating in diffusion and afterburning (DAB) mode. To date numerous experimental studies on the ejector have been carried out ranging from mixing only operation (Fabri and Paulon [3], Lineberry and Landrum [4], Quinn [5]) to those including the effects of combustion in either the SMC mode (Masuya et al. [6], Jos et al. [7], Li et al. [8]) or in DAB (Lehman et al. [9]). Many of these studies have been focused on improving the mixing process within ejectors due to its importance. For example, mixing can be improved by inducing large scale axial vortices inside an ejector by using either a hypermixing nozzle (Bevilaqua [10], Fancher [11], Quinn [12]) or forced mixer lobes (Presz et al. [13], Tillman et al. [14]). Another method is to use a dual thruster arrangement which was shown to

significantly improve mixing and air entrainment for an ejector under SMC operation (Cramer et al. [15]).

Modern computational methods have also been used to study ejectors under various operating conditions. Work in this area generally involves the solution of the averaged (Reynolds or Favre) Navier–Stokes equations coupled with eddy viscosity based turbulence models. When considering mixing without combustion computational simulations have been used to demonstrate methods for improving performance such as injecting the rocket exhaust around the annulus of the ejector (Etele and Sislian [16]) or by forcing the primary jet flow direction to oscillate (Daines and Bulman [17]). To simulate ejector operation under more detailed conditions the effects of combustion can also be included. This influences both the mixing rate and degree to which atmospheric air is entrained into the engine, especially under SMC conditions (Daines and Russel [18]). In fact, it has been shown both computationally (Daines and Segal [1]) and theoretically (Dobrowolski [19]) that DAB tends to perform significantly better than SMC unless specific modifications are made to the ejector to delay the combustion process (Russel et al. [20]).

One of the key influences on ejector performance is the quantity of entrained, or secondary, fluid that is obtained under a given set of conditions. To calculate this value many of the theoretical treatments of ejector systems assume that initially the primary and secondary streams do not mix and that the secondary stream chokes (Aoki et al. [21], Dutton and Carrol [22], Dutton et al. [23], Fabri and Paulon [3], Mikklesen et al. [24]). Further refinements to this approach can involve the calculation of a limited amount of mass transfer between streams up to the choke point (Chow and Addy [25]) or the effects of viscosity and heat transfer on the development of the shear layer (Papamoschou [26]). Alternatively, if one assumes that some uniform flow condition at the exit of the ejector section is known (such as Mach number or static pressure) then this information can be used to calculate the entrained flow rate without the need to specify how the two streams initially interact (Han et al. [27], Etele et al. [28]). However, without knowing the wall pressure distribution within the ejector, all of these methods are limited to constant area sections. Therefore, researchers have developed modified analyses in an effort to incorporate either experimental wall pressure data (Masuya et al. [6]) or approximations for the pressure variation within the ejector (Dobrowolski [19]).

This paper outlines a method capable of considering both the effects of variable area and combustion on the compression factor within an ejector without the need for experimental data. This is done by approximating the wall pressure with a function that qualitatively matches that produced by the effects of the shock structure within the supersonic primary stream. In addition, combustion effects are considered through the implementation of a chemical equilibrium calculation (similar to the work of Vanka et al. [29], Peters et al. [30], and Masuya et al. [6]). This allows the assessment of the effects due to both thermal choking as well as gas composition to be considered.

Theory

The solution procedure is based on previous work [28] which considers a quasi-one-dimensional flow through the control volume shown in Fig. 1. The flow conditions of the primary rocket stream entering the ejector at plane i are completely specified (T_r^o, p_r^o, and M_r) along with the chemical composition of the fluid (Y_r and thus both γ_r, and R_r). The flow conditions of the secondary, or entrained airstream, are set so as to reflect the atmospheric flight conditions (T_a^o, p_a^o, γ_a, R_a) but do not require one to set the massflow of entrained air entering the ejector. Instead, this value is obtained through the calculations and the solution is closed by specifying the pressure at the ejector mixed flow plane. Since the properties at the mixed flow plane are assumed uniform, this implies complete mixing is obtained at this location (generally requiring an ejector duct length on the order of 5 times the inlet diameter depending on the rocket configuration used). If the rocket area and ejector geometry are specified ($\sigma, A(x)$) then the conservation of mass through the control volume can be expressed as

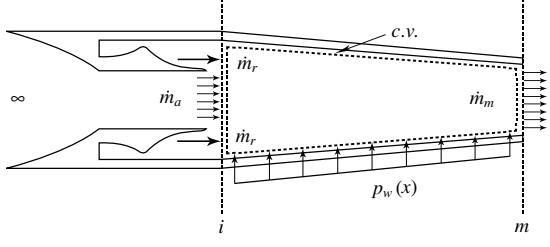

Fig. 1 Ejector control volume.

$$\dot{m}_r(\alpha+1) = p_m A_m \sqrt{\frac{\gamma_m}{R_m T_m^o}} M_m \sqrt{1+\frac{\gamma_m-1}{2}M_m^2} \tag{1}$$

where

$$\alpha = \dot{m}_a/\dot{m}_r \tag{2}$$

Under the given conditions this expression contains three unknowns. The Mach number at the ejector mixed flow plane M_m, the entrainment ratio α whose value is directly related to the Mach number of the entrained airflow at the ejector inlet plane M_a, and the total temperature at the ejector mixed flow plane T_m^o. Applying the conservation of momentum to the control volume in Fig. 1 while assuming inviscid flow can yield the following expression

$$M_m^2 = \frac{1}{\gamma_m}\left[\frac{\dot{m}_r a_r^*}{p_m A_m}(\alpha\sqrt{\theta}\Gamma\chi_a + \chi_r) - F_{p,x} - 1\right] \tag{3}$$

where θ and Γ are defined as

$$\theta = \frac{C_{p,a}T_a^o}{C_{p,r}T_r^o}, \qquad \Gamma = \sqrt{\frac{(\gamma_a-1)(\gamma_r+1)}{(\gamma_a+1)(\gamma_r-1)}} \tag{4}$$

and the sound speed at sonic conditions is simply

$$a^{*2} = 2\frac{\gamma-1}{\gamma+1}C_p T^o \tag{5}$$

In this expression both χ_a and χ_r are functions of the particular stream entering the ejector duct

$$\chi(\gamma, M) = \left[\frac{M+\frac{1}{\gamma M}}{\sqrt{\frac{2}{\gamma+1}+(\frac{\gamma-1}{\gamma+1})M^2}}\right] \tag{6}$$

and the term $F_{p,x}$ is the dimensionless wall pressure force (which reflects the influence of a changing area on the momentum of the flow within the ejector)

$$F_{p,x} = \frac{1}{p_m A_m}\int_0^L p_w(x)\cdot \mathrm{d}\mathbf{S}_x \tag{7}$$

Leaving $F_{p,x}$ for the moment, Eq. (3) is a function with only two unknowns, M_m and M_a (through α). Therefore, for a constant area ejector in which $F_{p,x} = 0$, if the flow is assumed steady, inviscid, and adiabatic then the total temperature at plane m can be expressed as

$$T_m^o = (C_{pm}[\alpha+1])/(\alpha C_{pa}T_a^o + C_{pr}T_r^o) \tag{8}$$

and thus Eqs. (1) and (3) can now be solved for the air entrainment Mach number and the resulting mixed flow Mach number that corresponds to the given flight conditions and ejector back pressure. However, to account for the possibility of simultaneous mixing and combustion within the ejector Eq. (8) cannot be applied and thus for a chemically reacting system the energy equation can be written as

$$\sum_{k=1}^{n_s} N_k\left[\bar{h}_k + W_m\frac{u_m^2}{2}\right] = \dot{m}_a h_a^o + \dot{m}_r h_r^o \tag{9}$$

where n_s is the number of atomic species being considered. The enthalpy terms in Eq. (9) can be expressed relative to a reference state to yield

$$h^o = \sum_{k=1}^{n_s} \frac{Y_k}{W_k} \bar{h}_{f,k} + C_p(T^o - T_{\text{ref}}) \tag{10}$$

while to simplify the kinetic energy term on the left side of Eq. (9) the ideal gas law and the speed of sound can be used to yield

$$W_m \frac{u_m^2}{2} \sum_{k=1}^{n_s} N_k = \frac{1}{2} \gamma_m N_m R_u T_m M_m^2 \tag{11}$$

Substituting Eqs. (10) and (11) into Eq. (9) while invoking the definitions of α and θ and noting that $N_m R_u = N_m W_m R_m = \dot{m}_m R_m$

$$\sum_{k=1}^{n_s} N_k \bar{h}_k + \frac{1}{2} \gamma_m \dot{m}_m R_m T_m M_m^2 = H \tag{12}$$

where H represents the total energy flowing into the ejector

$$H = \dot{m}_r \left[C_{p,r} T_r^o (\alpha\theta + 1) + \sum_{k=1}^{n_s} \frac{Y_{r,k}}{W_k} \bar{h}_{f,k} - T_{\text{ref}} (\alpha C_{p,a} + C_{p,r}) \right] \tag{13}$$

Equation (12) is the nonadiabatic equivalent of Eq. (8). This cannot be used to directly relate T_m^o to M_a as was the case with Eq. (8) due to the additional unknowns $\sum N_k$. However, assuming the flow at the ejector mixed flow plane is in chemical equilibrium allows one to solve Eq. (12) using the Gibbs Minimization technique. Additional properties at the ejector mixed flow plane can then be calculated using mass averaging and the ideal gas law

$$C_{pm} = \sum_{k=1}^{n_s} Y_k C_{pk}, \qquad W_m = \sum_{k=1}^{n_s} \frac{Y_k}{W_k}, \qquad \gamma_m = (1 - R_m / C_{pm})^{-1} \tag{14}$$

Although this is enough to solve for a chemically reacting constant area ejector, to extend the theory to variable area ejector ducts a wall pressure distribution is required for $F_{p,x}$ [Eq. (7)]. In this work the fourth-order polynomial shown in Eq. (15) is used

$$p_w(x) = p_{\min} + c_1 (c_2 - (x/L - 1)^2)^2 \tag{15}$$

This qualitatively mimics the pressure felt along the wall due to the expansion/compression process created by the shock train within the supersonic primary stream. This pattern can be observed for primary rocket streams located along the central axis of an axisymmetric configuration and those with an annular rocket configuration (Desevaux and Lanzetta [31], Aoki et al. [21], Kim and Kwon [32]). However, this work will assume an annular rocket configuration as this has been shown to produce better mixing within a given ejector length. For cases in which this pattern is not observed care should be exercised in applying this equation.

The constants c_1 and c_2 are found by applying the pressure boundary conditions along the wall within the control volume (i.e., $p_w(0) = p_r$, $p_w(L) = p_m$)

$$c_2 = (1 + \sqrt{\beta})^{-1} c_1 = (p_m - p_{\min}) / c_2^2 \tag{16}$$

where

$$\beta = (p_r - p_{\min}) / (p_m - p_{\min}) \tag{17}$$

The parameter $p_{\min}$ represents the minimum pressure to which the rocket exhaust expands and is found by considering only a small portion of the ejector duct from the inlet i, to the location at which the primary rocket stream expands to its lowest pressure x_2. If no mixing is assumed to occur within this length and a control volume is drawn around each stream then the conservation of momentum leads to

$$(\chi_r - \chi_{r2}) + \alpha \sqrt{\theta} \Gamma (\chi_a - \chi_{a2}) - F_{p,x_2} = 0 \tag{18}$$

where

$$F_{p,x_2} = \frac{1}{\dot{m}_r a_r^*} \int_0^{x_2} p_w(x) \cdot \mathrm{d}\mathbf{S}_x \tag{19}$$

The term F_{p,x_2} is similar to Eq. (7) but is integrated only up to the point where the rocket stream reaches its minimum pressure. The axial location of this point can be obtained directly from Eq. (15) by minimizing the expression and using the positive root to give

$$x_2/L = 1 - \sqrt{c_2} \tag{20}$$

Equations (15) and (20) can be substituted into Eq. (19) and integrated to obtain a closed form expression in terms of the constants c_1 and c_2 [in the same fashion as for Eq. (7)]. The continuity expression for the control volumes surrounding each of the streams up to point x_2 can be combined to yield

$$A_a(\mu_a/\mu_{a2}) + A_r(\mu_r/\mu_{r2}) = A(x_2) \tag{21}$$

where

$$\mu(\gamma, M) = \sqrt{\gamma} M (1 + [(\gamma - 1)/2] M^2)^{\frac{-(\gamma+1)}{2(\gamma-1)}} \tag{22}$$

Equations (18) and (21) contain a total of four unknowns (M_a, M_{a2}, M_{r2}, and $p_{\min}$) when trying to solve for the minimum pressure. However, if one assumes isentropic flow within the distance from i to x_2 then the minimum pressure can be found from p_r^o and M_{r2}. Therefore, the overall solution procedure involves first guessing at the value for M_a. This then allows Eqs. (18) and (21) to be used to solve for the Mach numbers at x_2 and thus the minimum pressure to which the primary rocket stream expands, $p_{\min}$. This then fixes $F_{p,x}$ within the variable area ejector duct. Using the guessed value for M_a one can determine the oxidizer to fuel ratio within the ejector duct while guessing a value for M_m allows the Gibbs Minimization technique to be used to obtain values for the mixed flow properties T_m and N_ks. Once the mixed flow composition and total temperature have been obtained, along with the dimensionless wall pressure force, Eqs. (1) and (3) can be solved and the resulting entrained air Mach number M_a and mixed flow Mach number M_m can be compared with the original guesses. This process can be repeated until converged values of these Mach numbers are obtained.

Results

Minimum Pressure

Previous numerical simulations done by the authors have considered a nonreacting flowfield within an axisymmetric ejector with a converging area and an annular rocket configuration as shown in Fig. 1. These configurations were solved using the axisymmetric, multispecies, Favre-averaged Navier–Stokes (FANS) equations combined with the Wilcox $k\omega$ turbulence model (including the Wilcox dilatational dissipation correction) in generalized curvilinear form using WARP [33] (window allocatable resolver for propulsion). This codes uses an implicit Euler time marching scheme incorporating block implicit factorization to iterate toward a steady-state solution using a pseudo time step determined from a combination of both the minimum and maximum Courant–Friedrichs–Lewy-based local time step conditions. The convective terms are treated using the Roe scheme in conjunction with Yee flux limiters while the diffusive terms are treated with a second order accurate, centered, finite differencing stencil. Convergence is judged against the magnitude of both the continuity and energy residuals. Details of the form of the flux vectors and the validation of this code on other high speed flows can be found in Parent and Sislian [34].

The results from one of these simulations will be used to test the accuracy of using the wall pressure profile defined by Eq. (15). The computational fluid dynamics (CFD) wall pressure profile shown in Fig. 2 corresponds to the set conditions listed in Table 1 for a kerosene fueled rocket within the ejector. This ejector geometry has a

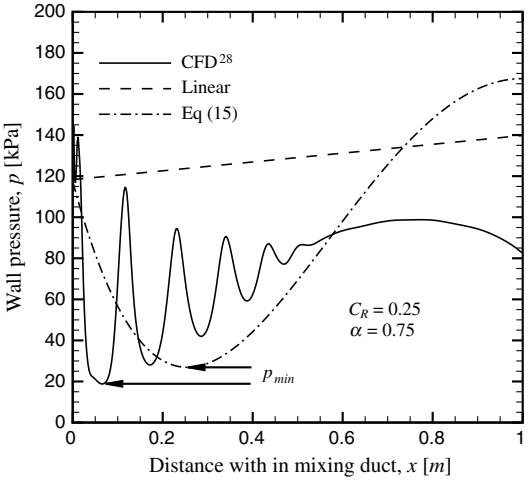

Fig. 2 Wall pressure distributions.

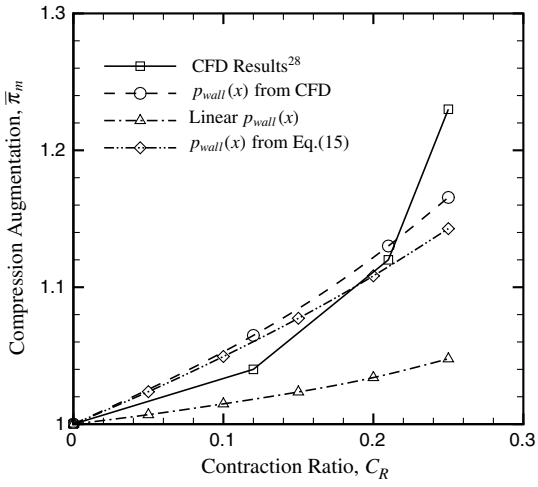

Fig. 3 Ejector compression augmentation $\bar{\pi}_m$.

mixed flow plane area that is 75% of the total inlet area and results in an approximately uniform mixed flow with a Mach number of unity within a length equal to 5 times the inlet diameter. Therefore, under the given conditions the ejector is operating at the maximum air massflow possible with an entrainment ratio of $\alpha = 0.75$. At the ejector inflow plane the static pressure ratio between the two streams is approximately 2 and thus the rocket stream quickly expands into the entrained air. This produces the pattern of expansion and compression in the wall pressure up to approximately $x = 0.5$ m seen in the CFD results. As shown, the lowest pressure produced by this flowfield is approximately 20 kPa (an 83% drop in pressure from the inlet conditions). Comparing this to the wall pressure distribution obtained using the approximation in Eq. (15) (when setting the mixed flow pressure so as to obtain the same entrainment ratio of 0.75) one can see that the minimum pressure is approximately 25 kPa (a 79% drop in pressure).

The reason for this difference is related to the shear layer, which allows for some fluid transfer between the two streams through mixing. This process is inherently nonisentropic and thus the total pressure within each stream decreases, a phenomenon that is modeled within the CFD simulations. However, up to the minimum pressure point (x_2) the theoretical analysis assumes isentropic flow and that no mixing occurs between the rocket and air streams. Although there exists a 4% difference in the predicted percentage pressure drop, of greater importance is the effect this has on changing the integrated value of the wall pressure on $F_{p,x}$ and the resulting effect on the calculated values of M_a and M_m (which are then used to define various ejector performance parameters like the compression augmentation and the entrainment ratio). Since the mixed flow plane pressure is a set variable it is possible to use a linear wall pressure distribution (also shown in Fig. 2). In this case the wall pressure starts at the same initial pressure as the other profiles and increases to the mixed flow pressure required to obtain an entrainment ratio of 0.75. Since the mixed flow pressure is higher than that at the inlet, this profile is incapable of predicting the initial pressure drop and will thus allow an assessment of the importance of modeling this effect on overall ejector performance.

Ejector Compression Augmentation

Given that one of the main benefits of using a constricting area ejector is to increase the compression ratio obtained at the mixed flow plane, the compression augmentation $\bar{\pi}_m$ will be used to evaluate any improvements in performance. This configuration requires the wall pressure to be considered and so three methods will be compared. The simplest approach is to use a linear wall pressure distribution in the theoretical analysis. Alternatively one can use Eq. (15) to more accurately reflect the wall pressure conditions. In cases where experimental or computational wall pressure distributions are available, it is also possible to use this information in the theoretical analysis through numerical integration of Eq. (7) (this represents the limit in terms of accuracy for the theoretical model with wall pressure effects included). All three of these approaches are used and their effects on the compression augmentation achieved for various degrees of area constriction are shown in Fig. 3. It should be noted that compression augmentation can also be influenced by changing the entrainment ratio, therefore, in all cases shown the mixed flow plane pressure is varied so as to obtain $\alpha = 0.75$ for all the contraction ratios considered.

As can be seen, using the profile as defined by Eq. (15) yields a trend that is in good agreement with that obtained when integrating the wall pressure distribution extracted from the CFD results (thereby including all the pressure variations within the shock train region). Therefore, although there exists a larger difference between the $p_{\min}$ predicted using the method described above and that observed in the CFD simulation, the resulting effect on the overall compression augmentation is not as significant. The same cannot be said about the linear pressure variation, where as can be seen the trend with increasing contraction does not match well with the others, indicating that ignoring the influence of the expansion/compression process within the supersonic primary stream on the wall pressure creates a significant error for variable area ejectors. In addition to the trends predicted by the theoretical analysis, the compression augmentation as calculated directly from the CFD simulations at the mixed flow plane is shown. The width of the mixing zone at the ejector mixed flow plane in the CFD simulations is observed to extend across the entire height of the ejector thereby producing a significant degree of turbulent flow. However, the theoretical analysis does not include any effects due to turbulence, which contributes to differences observed between even the CFD compression augmentation trend and the trend calculated using the theoretical analysis and the CFD wall pressure distribution. In addition, any degree of non uniformity at the ejector mixed flow plane would contribute to a difference between the CFD and theoretical predictions. However, in the CFD simulations the flow is found to be 93% mixed at the ejector mixed flow plane based on an outflow mixing parameter which considers the curvature of the velocity profile.

Table 1 Ejector configuration for CFD results [28]

T_r^o	p_r^o	T_a^o	p_a^o
2316 K	58.7 atm	279 K	0.58 atm
M_r	σ	C_R	L/D
3.1	0.1	0.25	5

Effects of Combustion

The previous results are for an ejector in which there is no combustion or heat release past the ejector inlet plane. For this to

Table 2 Simultaneous mixing and combustion conditions

M_r	p_r^o	T_a^o	p_a^o
3.1	58.7 atm	279 K	0.58
σ	L/D	C_R	ϕ_R
0.1	5	0.15	0.2–2.5

Table 3 Species used in the Gibbs Minimization technique

CO_2	CO	CH_3	CH_4	C_2H_2	C_2H_4
O_2	O	OH	N_2	N	NO
H_2O	H_2	H	HO_2	H_2CO	

occur requires that there are no species within the primary rocket stream as it enters the ejector that can react with the oxygen within the secondary entrained airstream to release heat. To achieve this, the equivalence ratio within the rocket chamber must be set below the values used in typical rocket applications (for the CFD simulations this value is set to $\phi = 0.2$). If the equivalence ratio within the rocket chamber is increased then the effects of secondary combustion within the ejector mixing duct should be considered. To evaluate this effect the ejector configuration studied previously with a contraction ratio of $C_R = 0.15$ will be evaluated while varying the equivalence ratio in the rocket combustion chamber (see Table 2). For each equivalence ratio considered, the mixed flow pressure p_m is varied so that in all cases an entrainment ratio of $\alpha = 0.75$ is maintained. When calculating the equilibrium composition of the primary rocket stream entering the ejector and that of the mixed flow, they are assumed to be composed of some combination of the species listed in Table 3.

Figure 4 shows the compression augmentation factor normalized by the value at a contraction ratio of 0.15 and with no combustion within the ejector duct ($[\pi_m]_{\phi_r=0.2}$). As can be seen, increasing the equivalence ratio within the rocket combustion chamber will actually decrease the compression augmentation obtained for all values less than $\phi = 2$. This is significant in that most rocket applications operate at equivalence ratios above unity. This implies that any theoretical estimates of compression augmentation within the ejector that do not account for the possible effects of simultaneous mixing and combustion will overestimate the performance at or near nominal operating conditions. Under fuel rich conditions neglecting the additional combustion within the ejector mixing section will underestimate the compression augmentation.

Since the compression within the ejector is a measure of the total pressure at the mixed flow plane, Fig. 5 shows how both the static pressure and the Mach number at this plane vary as the equivalence ratio is altered. For each curve the percentage change from the maximum is plotted. In the case of the static pressure the maximum

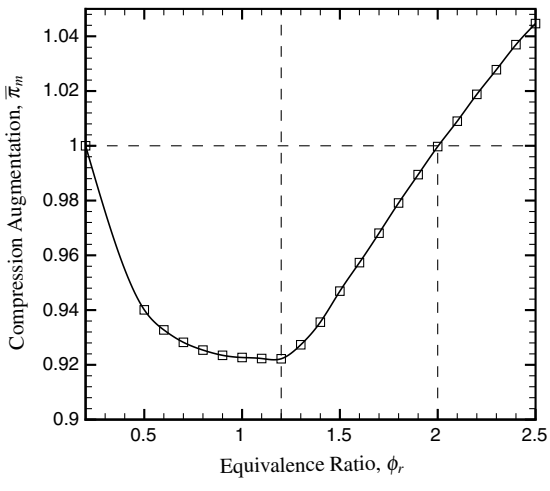

Fig. 4 Compression augmentation for SMC ($C_R = 0.15$, $\alpha = 0.75$).

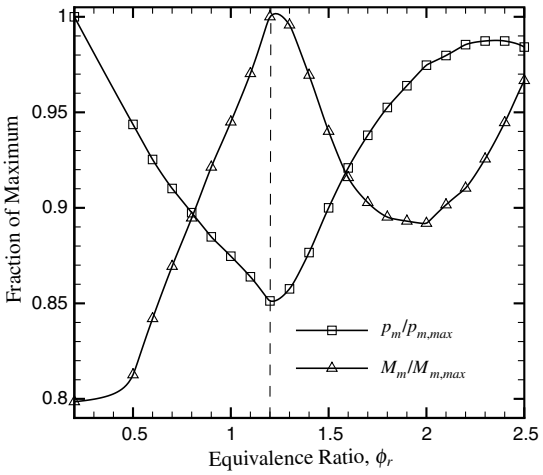

Fig. 5 Change in pressure and Mach number for SMC ($C_R = 0.15$, $\alpha = 0.75$).

mixed flow pressure is obtained at $\phi = 0.2$ when operating at $\alpha = 0.75$, while for the Mach number the maximum occurs at $\phi = 1.2$ at the same entrainment ratio. Comparing Figs. 4 and 5 one can see that the compression augmentation curve follows the same trend as that seen for the static pressure at the mixed flow plane. This indicates that although the Mach number at the mixed flow plane increases between an equivalence ratio of 0.2 and 1.2 (which would tend to increase p_m^o), the effect of a lower static pressure decreasing the total pressure is the dominant factor. Past $\phi = 1.2$ the mixed flow static pressure begins to rise and is within 3% of the maximum pressure at an equivalence ratio of 2. This condition, combined with an increasing Mach number above $\phi = 2$, leads to the increased compression augmentation shown in Fig. 4 for $\phi > 2$. These results indicate that ejector compression can be increased through area constriction provided a minimum equivalence ratio is used which is slightly above normal operating values. Further increases in compression can be obtained through greater increases in the equivalence ratio past this value (up to the choked flow condition for the given entrainment ratio).

These results account for changes in the ejector compression as a result of two distinct effects. First, changing the equivalence ratio will change the primary rocket stream conditions entering the ejector (T_r^o and γ_r) which will effect $\bar{\pi}_m$ even in the absence of further (secondary) combustion within the ejector duct. Second, as ϕ changes the resulting equilibrium composition of the primary rocket stream entering the ejector will change ($\sum_k N_k$) and thus could lead to secondary combustion (simultaneous mixing and combustion). Therefore, it is helpful to distinguish these two processes and their relative impact on the compression augmentation.

Figure 6 shows the compression factor of the ejector for various equivalence ratios. For the curve with primary combustion alone, even though the rocket stream entering the ejector may contain species capable of reacting with the entrained air to release heat, these reactions are not considered. At low equivalence ratios there is little difference between the two curves. At stoichiometric conditions, if secondary combustion is not accounted for, the resulting compression factor at the mixed flow plane is over estimated by approximately 3%. Given that the effect of varying the equivalence ratio on the compression factor is 8% or less as shown in Fig. 4, neglecting the effect of secondary combustion can reduce the accuracy of the results by 40% or more. This difference is the greatest at stoichiometric conditions, however, even as the equivalence ratio is increased to values above 2 there remains a significant difference between calculations done with and without considering the effects of secondary combustion. For example, operating the primary rocket at an equivalence ratio of 2.5, Fig. 4 indicates that the resulting compression factor can be increased 4% above what one would obtain under conditions where no secondary combustion is occurring. However, if the secondary combustion effects are not

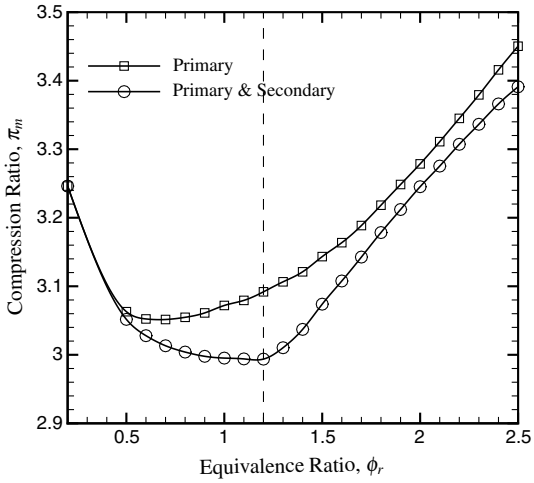

Fig. 6 Ejector compression ($C_R = 0.15, \alpha = 0.75$).

accounted for at this equivalence ratio, Fig. 6 indicates that the resulting compression factor will be over predicted by approximately 1.7%, or over 40% of the expected increase.

Conclusions

A theoretical formulation for a variable area ejector is presented which accounts for both wall pressure effects and the effects due to simultaneous mixing and combustion within the ejector. An analytical pressure distribution which qualitatively mimics the effects of the expansion/compression process within the supersonic primary rocket stream on the wall pressure is shown to produce results similar to those obtained using extracted pressure distributions from CFD simulations. This pressure distribution does not require any additional information about the flow other than that already required to solve for the ejector performance, and is shown to significantly improve the accuracy when compared with a simple linear wall pressure approximation.

Results show that area constriction can be used to increase the compression factor within an ejector, but that this increase is sensitive to the equivalence ratio of the primary rocket stream. For a given area constriction, the results show that compression augmentation is highest at both fuel lean and fuel rich conditions, while at equivalence ratios typical of kerosene/oxygen rockets the compression augmentation is near a minimum. An area constriction of 15% is shown to be capable of an approximate 8% increase in the compression factor of the ejector at an equivalence ratio of both 0.2 at 2, however, under the same conditions an equivalence ratio of 1.2 decreases the compression factor by the same amount. It is also shown that these results are not due solely to the change in the properties of the primary rocket exhaust entering the ejector (such as total temperature or ratio of specific heats). Assuming chemical equilibrium of a total of 17 species at the mixed flow plane, it is shown that nearly half of the effect of changing the equivalence ratio is due to the presence of secondary combustion occurring within the ejector.

Acknowledgment

This work was sponsored by the Natural Science and Engineering Research Council of Canada.

References

[1] Daines, R., and Segal, C., "Combined Rocket and Airbreathing Propulsion Systems for Space-Launch Applications," *Journal of Propulsion and Power*, Vol. 14, No. 5, 1998, pp. 605–612. doi:10.2514/2.5352

[2] von Karman, T., "Theoretical Remarks on Thrust Augmentation," *Reissner Anniversary Volume: Contributions to Applied Mechanics*, edited by P. I. of Brooklyn, J. W. Edwards, Ann Arbor, Michigan, 1949, pp. 461–468.

[3] Fabri, J., and Paulon, J., "Theory and Experiments on Supersonic Air–Air Ejectors," NACA, Tm-1410, 1956.

[4] Lineberry, D., and Landrum, B., "Effects of Multiple Nozzles on Asymmetric Ejector Performance," AIAA, Paper 2005-4283, 2005.

[5] Quinn, B., "Ejector Performance at High Temperatures and Pressures," *Journal of Aircraft*, Vol. 13, No. 12, 1976, pp. 948–954. doi:10.2514/3.44561

[6] Masuya, G., Chinzei, N., and Ishii, S., "A Study of Airbreathing Rockets—Subsonic Mode Combustion," *Acta Astronautica*, Vol. 8, Nos. 5–6, 1981, pp. 643–661. doi:10.1016/0094-5765(81)90110-7

[7] Jos, C. C., Anderson, W. E., Sankaran, V., and Gujarathi, A., "Ducted Rocket Tests with a Fuel Rich Primary Thruster," AIAA Paper 2005-4282, 2005.

[8] Li, Y. F., He, G. Q., and Liu, P. J., "Experimental Investigation of Rocket Ejector in SMC Combustion Mode," AIAA Paper 2006-5042, 2006.

[9] Lehman, M., Pal, S., and Santoro, R. J., "Experimental Investigation of the RBCC Rocket- Ejector Mode," AIAA Paper 2000-3725, 2000.

[10] Bevilaqua, P. M., "Evaluation of Hypermixing for Thrust Augmenting Ejectors," *Journal of Aircraft*, Vol. 11, No. 6, 1974, pp. 348–354. doi:10.2514/3.59257

[11] Fancher, R. B., "Low-Area Ratio, Thrust-Augmenting Ejectors," *Journal of Aircraft*, Vol. 9, No. 3, 1972, pp. 243–248. doi:10.2514/3.58964

[12] Quinn, B., "Compact Ejector Thrust Augmentation," *Journal of Aircraft*, Vol. 10, No. 8, 1973, pp. 481–486. doi:10.2514/3.60251

[13] Presz, W. M. J., Morin, B. L., and Gousy, R. G., "Forced Mixer Lobes in Ejector Designs," *Journal of Propulsion and Power*, Vol. 4, No. 4, 1988, pp. 350–355. doi:10.2514/3.23073

[14] Tillman, T. G., Paterson, R. W., and Presz, W. M., "Supersonic Nozzle Mixer Ejector," *Journal of Propulsion and Power*, Vol. 8, No. 2, 1992, pp. 513–519. doi:10.2514/3.23506

[15] Cramer, J. M., Greene, M., Pal, S., and Santoro, R. J., "RBCC Ejector Mode Operating Characteristics for Single and Twin Thruster Configurations," AIAA Paper 2001-3464, 2001.

[16] Etele, J., and Sislian, J. P., "Analysis of Increased Compression Factor on Ejector-Rocket Performance," ICAS Paper 2006-5.2.2, 2006.

[17] Daines, R. L., and Bulman, M., "Computational Analyses of Dynamic Rocket Ejector Flowfields," AIAA Paper 96-2686, 1996.

[18] Daines, R. L., and Russel, R. M., "Numerical Analysis of the Effects of Combustion in Rocket Ejectors," AIAA Paper 1998-3772, 1998.

[19] Dobrowolski, A., "Analysis of Nonconstant Area Combustion and Mixing in Ramjet and Rocket-Ramjet Hybrid Engines," NASA, Tn d-3626, 1966.

[20] Russel, R. M., Brocco, D. S., and Daines, R. L., "Modeling and Validation of an Ejector Primary Rocket for Shielded Afterburning Fuel Injection," AIAA Paper 99-2241, 1999.

[21] Aoki, S., Lee, J., and Masuya, G., "Aerodynamic Experiment on an Ejector-Jet," *Journal of Propulsion and Power*, Vol. 21, No. 3, 2005, pp. 496–503. doi:10.2514/1.6736

[22] Dutton, J. C., and Carrol, B. F., "Optimal Supersonic Ejector Designs," *Journal of Fluids Engineering*, Vol. 108, No. 4, 1986, pp. 414–420. doi:10.1115/1.3242597

[23] Dutton, J. C., Mikkelsen, C. D., and Addy, A. L., "A Theoretical and Experimental Investigation of the Constant Area, Supersonic–Supersonic Ejector," *AIAA Journal*, Vol. 20, No. 10, 1982, pp. 1392–1400. doi:10.2514/3.51199

[24] Mikklesen, C. D., Sandberg, J., and Addy, A., "Theoretical and Experimental Analysis of the Constant-Area, Supersonic–Supersonic Ejector," University of Illinois at Urbana-Champaign, Uilu-eng-76-4003, 1976.

[25] Chow, W. L., and Addy, A. L., "Interaction Between Primary and Secondary Streams of Supersonic Ejector Systems and Their Performance Characteristics," *AIAA Journal*, Vol. 2, No. 4, 1964, pp. 686–695. doi:10.2514/3.2403

[26] Papamoschou, D., "Analysis of a Partially Mixed Supersonic Ejector," *Journal of Propulsion and Power*, Vol. 12, No. 4, 1996, pp. 736–741. doi:10.2514/3.24096

[27] Han, S., Peddieson, J. J., and Gregory, D., "Ejector Primary Flow Molecular Weight Effects in an Ejector Ram-Rocket Engines," *Journal of Propulsion and Power*, Vol. 18, No. 3, 2002, pp. 592–599. doi:10.2514/2.5973

[28] Etele, J., Parent, B., and Sislian, J. P., "Analysis of Increased

Compression Through Area Constriction on Ejector-Rocket Performance," *Journal of Spacecraft and Rockets*, Vol. 44, No. 2, 2007, pp. 355–364.
doi:10.102514/1.26915

[29] Vanka, S., Craig, R., and Stull, F., "Mixing, Chemical Reaction, and Flowfield Development in Ducted Rockets," *Journal of Propulsion and Power*, Vol. 2, No. 4, 1986, pp. 331–338.
doi:10.2514/3.22891

[30] Peters, C. E., Phares, W. J., and Cunningham, T. H. M., "Theoretical and Experimental Studies of Ducted Mixing and Burning of Coaxial Streams," *Journal of Spacecraft and Rockets*, Vol. 6, No. 12, 1969, pp. 1435–1441.
doi:10.2514/3.29843

[31] Desevaux, P., and Lanzetta, F., "Computational Fluid Dynamic Modeling of Pseudoshock Inside a Zero-Secondary Flow Ejector," *AIAA Journal*, Vol. 42, No. 7, 2004, pp. 1480–1483.
doi:10.2514/1.1125

[32] Kim, S., and Kwon, S., "Starting Pressure and Hysteresis Behaviour of an Annular Injection Supersonic Ejector," *AIAA Journal*, Vol. 46, No. 5, May 2008, pp. 1039–1044.
doi:10.2514/1.22363

[33] Parent, B., and Sislian, J. P., "The Use of Domain Decomposition in Accelerating the Convergence of Quasi-Hyperbolic Systems," *Journal of Computational Physics*, Vol. 179, No. 1, 2002, pp. 140–169.
doi:10.1006/jcph.2002.7048

[34] Parent, B., and Sislian, J. P., "Validation of the Wilcox kw Model for Flows Characteristic to Hypersonic Airbreathing Propulsion," *AIAA Journal*, Vol. 42, No. 2, 2004, pp. 261–270.
doi:10.2514/1.1989

C. Segal
Associate Editor